JOURNAL OF MATERIALS SCIENCE 15 (1980) 739–746

Hertzian indentation of thorium dioxide, ThO_2

Hj. MATZKE
Commission of the European Communities Joint Research Centre, Karlsruhe Establishment, European Institute for Transuranium Elements, Postfach 2266, D-7500 Karlsruhe, West Germany

The Hertzian indentation technique was used to study the fracture properties of ThO_2 and to measure the fracture surface energy, γ, of sintered ThO_2. Optical microscopy and acoustic emission were employed to detect ring crack formation. Perfect cracks were always formed and no indication of permanent plastic deformation was observed. From the observed crack behaviour, a fracture surface energy, γ, of $2.5 \pm 0.2\,J\,m^{-2}$ at room temperature and a fracture toughness, K_{IC}, of $1.07\,MN\,m^{-3/2}$ were deduced.

1. Introduction

The fracture properties as well as the fracture surface energy of fluorite type nuclear materials such as UO_2, $(U, Pu)O_2$ or ThO_2 are interesting because of the application of these materials in nuclear reactors. To fully understand the cracking and fission gas swelling behaviour, relevant information on all these fuel materials is needed. Whereas deviations from the stoichiometric composition can greatly change the physical properties such as the surface energy of e.g. UO_2 [1–3], use of the more stable substance ThO_2 should avoid this difficulty. Therefore, experiments were performed with ThO_2. The method of Hertzian indentation was selected to obtain simultaneous information on fracture properties and fracture surface energy.

This method, originally described by Hertz [4], has recently been tested for its applicability to measure fracture surface energies [5–7]. In brief, when a spherical indentor is pressed onto the surface of a brittle elastic material, ring cracks form with radius r if the applied load surpasses a certain critical load P_c. Subject to certain conditions the Auerbach law [8] can be expected to hold, namely:

$$P_c = A \cdot R \qquad (1)$$

where the constant A can be shown to depend linearly on fracture surface energy, γ, (e.g. [10]). For ideally brittle materials, γ can thus be obtained from crack measurements [9]. The mathematics involved have recently been discussed (e.g. [5, 6, 11]). In particular, Warren [5] has shown that the ring crack is expected to form outside the area of contact between indentor and sample, a: according to this treatment, the Hertzian ring crack will first occur at a minimum load, P_c, independent of flaw size, provided there are flaws of size larger than a certain minimum size, c'', of about 0.01 to $0.03a$. This treatment in proposing a minimum flaw size avoids the objections of the "flaw statistical argument", according to which P_c would depend on flaw statistics, hence on the existence of particularly suitable flaws [12]. Previous work with this method to obtain information on fracture surface energies has dealt with ZrC, VC, WC [5], TiC [5, 13], NbC [7] and UO_2 [6].

2. Experimental details

Sintered discs of ThO_2 of density $9.2 \times 10^3\,kg\,m^{-3}$ (92% theoretical density) and an average grain size of $22\,\mu m$ were used. The surfaces were polished with diamond paste. Hertzian indentations were performed in a hardness testing machine (Frank) with hardened steel indentors at room temperature. A constant loading rate of $0.09\,mm\,sec^{-1}$ was used. For each indentation, the steel indentor was re-adjusted to give a fresh contact area. Following about 20 indentations, the indentors were replaced. Usually, kleenex or cotton-gloves were used to re-adjust the indentors. Sometimes, however, the indentors were intentionally rolled with a finger tip to apply a thin film of "grease" or "dirt" to facilitate detection of the contact area in the microscope. Following all indentations at one load (usually 4 to 5 indentations), the samples were

0022–2461/80/030739–8$02.80/0

examined in an optical microscope. If 2 out of 4 indentations yielded ring cracks, or if the cracks approached 50% of a full circle, the load was taken as critical load, P_c. In general, the range between the load, where no cracks were observed, and the load, where 4 cracks out of 4 indentations were observed, was $\leqslant 10\%$ of P_c. When ring cracks formed, their radii were measured in the microscope. Similarly, when a thin "dirt" layer was applied to the indentor, the "dirt" rings produced during indentation were measured. In some cases, an acoustic emission apparatus especially developed for crack and fracture detection (Dunegan/Endevco) was used to measure integrated noise pulses at a frequency of 155 kHz. The noise level (number of counts) due to application of subcritical loads was very small, whereas crack formation could easily be detected since it led to a significantly higher number of pulses.

3. Principles of the method

Hertz [4] has shown that the area of contact between the indentor and specimen is given by

$$a^3 = 4kPR/3E \qquad (2a)$$

with

$$k = \tfrac{9}{16}[(1-\nu^2) + (1-\nu'^2)E/E']$$

where a is the radius of circle of contact, R the radius of indentor, ν Poisson's ratio of the specimen, E the elasticity or Young's modulus of the specimen, and ν' and E' Poisson's ratio and Young's modulus of the indentor (hardened steel with $\nu' = 0.29$ and $E' = 2.1 \times 10^{11}\ \mathrm{N\,m^{-2}}$). The experimental arrangement is schematically shown in Fig. 1. The crack radius r is usually slightly larger than a, hence the cracks are formed outside the area of contact. They extend to a depth c in a cone-shaped form. The pores in the sintered specimens had sizes in the range of 1 to 20 μm and were thus of suitable size, c_f. The "grease" or "dirt" ring, whenever formed, was expected, and found to be slightly outside the area of contact.

In the treatment of Warren, the curve of load P versus the ratio of crack length, c, to radius of contact circle, a, does not have two minima as proposed in previous work [14] but rather only one minimum and therefore one critical load, P_c at crack depth c''. Warren [5] shows that Auerbach's law can then be written as follows:

$$P_c = \beta \frac{kR\gamma}{(1-\nu^2)} \cdot \frac{a}{c''} [\phi'']^{-2} \qquad (3)$$

where ϕ denotes the integral, over the crack path, of the variable principle tensile stress normal to the crack path (see [5] for details) and β is a constant. If it is assumed, that the cone crack has the same stress intensity factor as a plane, internal crack of length, $2c$, then the value of β is $8\pi^3/27 = 9.18$. The integral or crack expansion function can be solved numerically [5] and depends on the

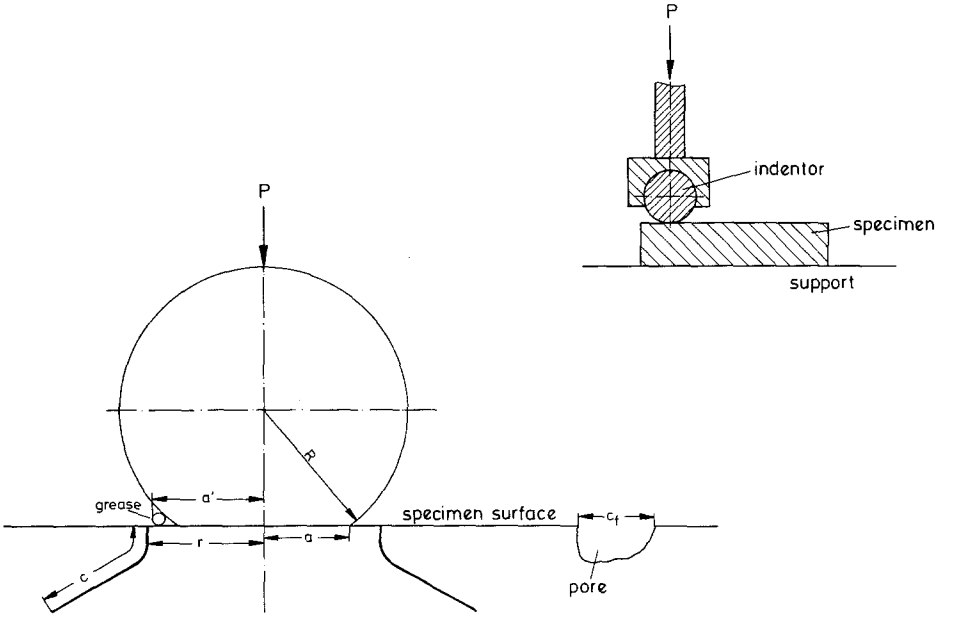

Figure 1 Schematic presentation of the geometry of Hertzian indentation cracking.

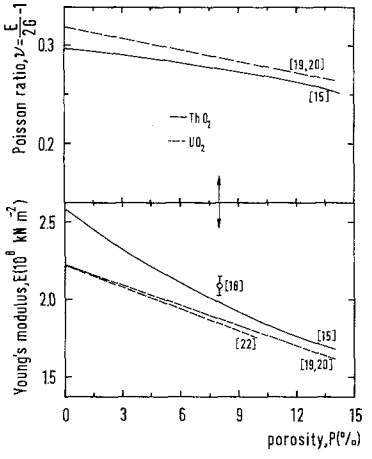

Figure 2 Poisson ratio, ν, and Young's modulus, E, for ThO_2 as function of porosity. The data for UO_2 are included for comparison.

location of the crack, r/a, and Poisson ratio, ν, of the specimen.

The literature on the elastic properties of ThO_2 [15–18] shows that ν depends on porosity* as reproduced in Fig. 2. The same is true for the Young's modulus, E, which is needed to calculate k and a. The porosity dependence of E is also shown in Fig. 2, where additional literature data for UO_2 are included [19–22]. UO_2 is isostructural with ThO_2 and is a well investigated material because of its wide use as fuel material in nuclear reactors. An arrow indicates the porosity of the ThO_2 used here. A direct determination of E on the actual samples of the present study was made by Dr C. Politis and yielded $E = (2.10 \pm 0.05) \times 10^{11}$ N m^{-2} [23]. This value was used for the present room temperature experiments together with a ν-value of 0.278. For this value of ν, the crack extension function $(a/c'')[\phi'']^{-2}$ as numerically integrated by Warren [5], is shown in Fig. 3. Obviously, its value depends strongly on the normalized size of the ring crack, r/a. It also depends strongly on ν, as is indicated at $r/a = 1.1$ in Fig. 3 for the range $0.25 \leqslant \nu \leqslant 0.30$. The total change involved can be of the order of a factor of 2.

Compared with this, the dependence of the other variables of Equation 3, i.e. k or $k/(1-\nu^2)$ on ν or E are less pronounced as is shown in Fig. 4, where these quantities are plotted as function of porosity. The total possible change is only of the order of 30% for reasonable variations in porosity.

The threshold crack length, c'', for the present case ($\nu = 0.278$, $r/a = 1.1$) is found from Warren's results [5] to be $\sim 0.03a$. With the a-values used (see Fig. 11) of $0.2\,\text{mm} \lesssim a \lesssim 0.4\,\text{mm}$, a critical flaw size of $6\,\mu\text{m} \leqslant c'' \leqslant 12\,\mu\text{m}$ would be required. The pore size in the ThO_2, as determined microscopically, was $10 \pm 5\,\mu$m and therefore enough suitable pores were available for crack formation even for the biggest indentors used.

4. Results

Indentations were performed using indentors with radii between 0.5 and 10 mm. Fig. 5 shows some typical ring cracks as observed in the optical microscope. At the critical load, very faint cracks formed which could be found by visual observation after some searching, but which were difficult to photograph. Slight mechanical polishing of the surface facilitated observation since small pieces were broken out from the edge of the ring crack. At increasing load, the ring became more obvious

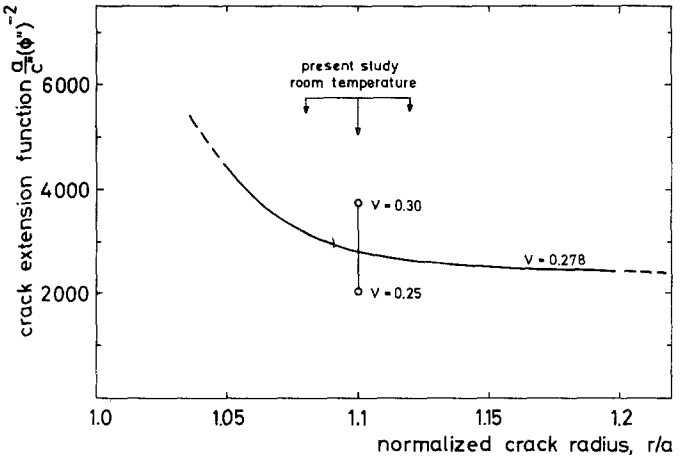

Figure 3 Crack extension function versus normalized crack radius, r/a, as calculated by Warren [5]. For a constant $r/a = 1.1$, the dependence on Poisson ratio, ν, is indicated.

* The effects of type of porosity (e.g. size, distribution), grain size and of metallic impurities are not known.

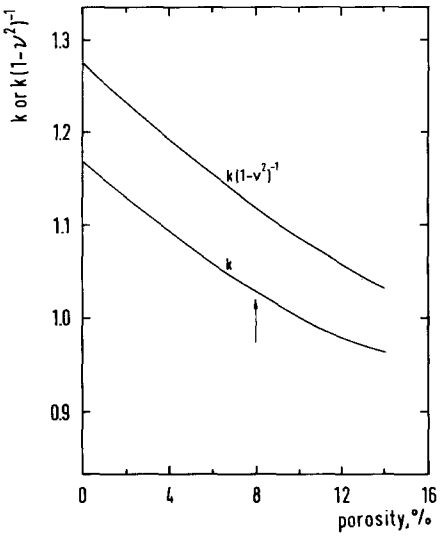

Figure 4 The dependence of k and $k/(1-\nu^2)$ for ThO_2 on porosity.

until at further increase, double or "overload" cracks appeared (Fig. 5d to f). Evidence for permanent plastic deformation was only observed for heavily overloaded small indentors ($R = 0.5$ and 1 mm) (Fig. 5e, f). At drastic overloading, radial cracks appeared in addition to the ring cracks (Fig. 5d to f). Fig. 6 gives a schematic presentation of the crack formation.

Before determining P_c as a function of R, a number of indentations were performed to compare "dirt" rings with the calculated contact area. As shown in Fig. 7, the "dirt" rings were slightly bigger than the contact area ($a'/a = 1.05 \pm 0.02$) and thus confirmed the accuracy of the calculated a-values.

In addition to visually observing crack formation, acoustic emission was used. Noise pulses at 155 kHz were integrated at different loads. Fig. 8

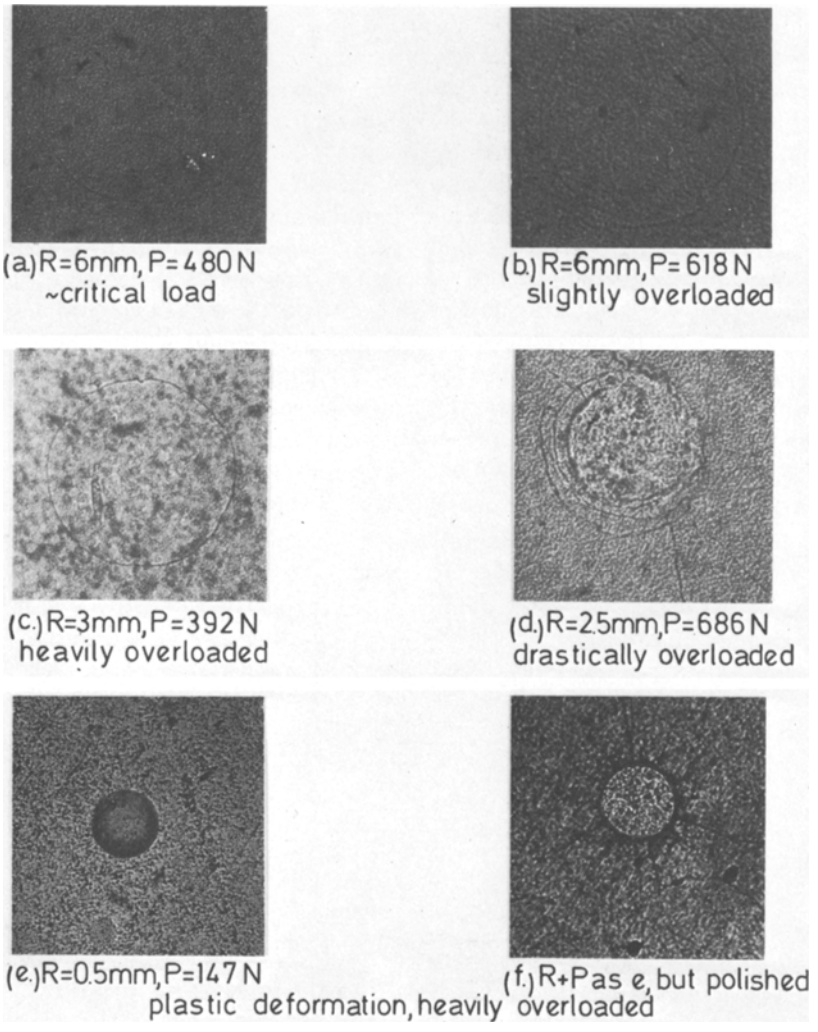

Figure 5 Optical micrographs of ring cracks in ThO_2 at various degrees of loading.

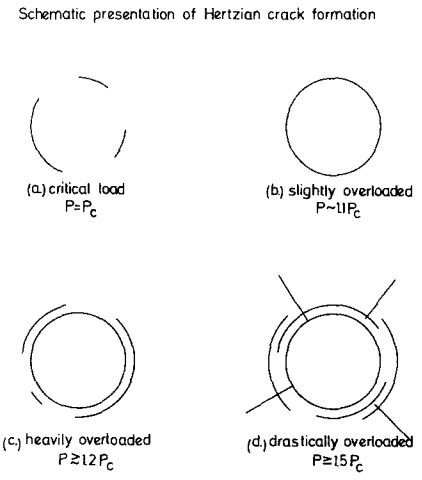

Figure 6 Schematic presentation of ring crack formation.

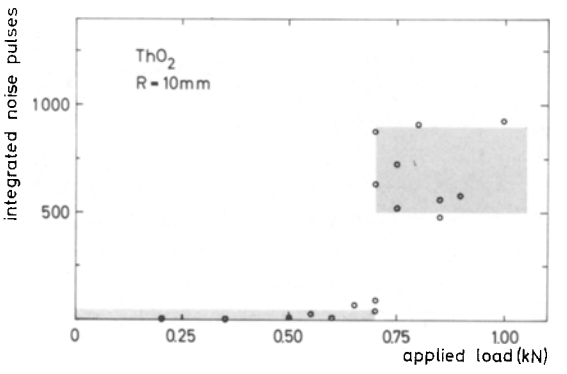

Figure 9 Acoustic emission during loading and crack formation with an indentator of $R = 10$ mm. P_c is obtained as 700 N.

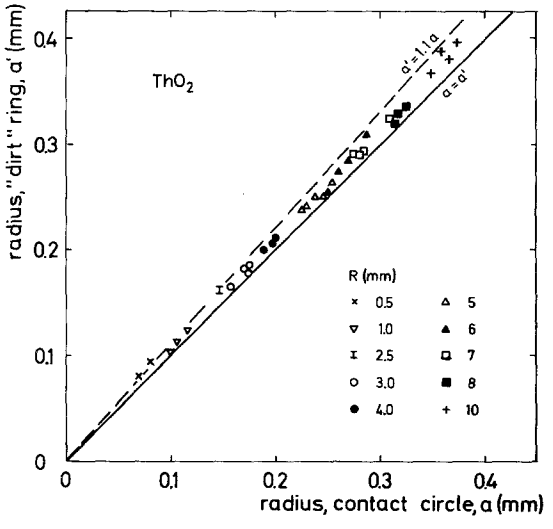

Figure 7 Measured "dirt" ring radii, a', versus calculated radii of the contact area, a, for different indentors (R from 0.5 to 10 mm).

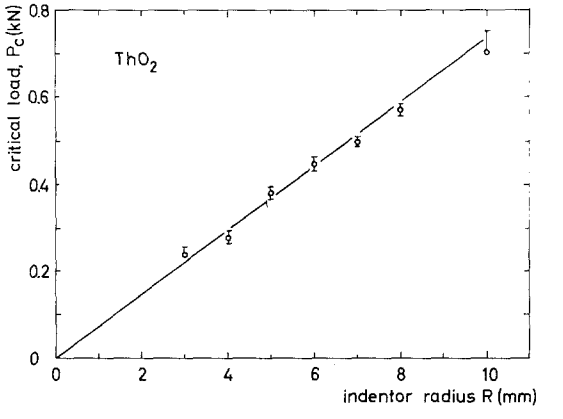

Figure 10 Critical cracking load, P_c, as function of indentor radius, R.

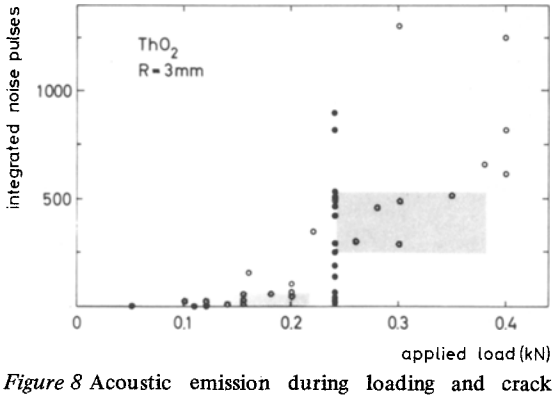

Figure 8 Acoustic emission during loading and crack formation with an indentor of $R = 3$ mm. P_c is obtained as 240 N.

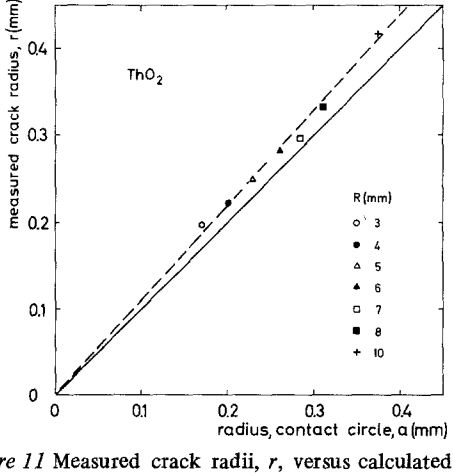

Figure 11 Measured crack radii, r, versus calculated radii of the contact area, a, for cracking at the critical load, P_c.

shows that, for an indentor of $R = 3$ mm, less than 100 integrated noise pulses were usually measured for loads < 200 N, whereas at least 300 pulses were always measured at loads $\geqslant 260$ N. At 240 N, which was taken as P_c, 8 loadings gave more than 300 pulses, 5 loadings less than 200 pulses. For high loads, double cracks ("overload" cracks as in Fig. 5) were observed with a high number of noise pulses. For $R = 10$ mm (see Fig. 9), the scatter is less. P_c is determined as 700 N, at which load 2 out of 4 indentations give more than 500 noise pulses, which is the level for crack formation observable in the microscope.

The acoustic emission data also served to define the time of crack formation. Noise pulses were always obtained as soon as the full load was applied (if $P \sim P_c$). Application of the load for a long time or unloading gave either zero noise or negligible noise pulses ($\leqslant 1\%$ of the total integrated sum).

Fig. 10 shows the critical crack load, P_c, at room temperature, as function of indentor radius, R. Auerbach's law is well confirmed, giving an Auerbach's constant $A = (73 \pm 3)\,\mathrm{kN\,m^{-1}}$.

To evaluate the fracture surface energy, γ, the normalized crack size, r/a, must be known (see Fig. 11). No information is available on whether or not (and how) r/a might vary with R or P. A number of indentations were therefore performed at constant R (5 mm). The cracks were much more easily visible and their radii could much better be measured following a slight polishing of the surface: about 10 μm of the surface were polished away with 1 μm diamond paste using a lapping device. The crack radii tended to be quite constant (see Fig. 12) indicating that the cracks were formed when the load approached the critical rather than the final value. At higher loads, overload (double) cracks were formed thus yielding more than one r-value. Also, for the range $3\,\mathrm{mm} \leqslant R \leqslant 10\,\mathrm{mm}$, all r/a-values were in the range $1.04 \leqslant r/a \leqslant 1.14$, with no apparent dependence on R. To evaluate r/a, it is important to decide whether the actual load or P_c should be used to calculate a. Whenever overloading is obvious, hence if concentric double cracks are observed, a meaningful unique r/a value cannot be obtained. For the cracks formed at the critical load, a range $1.07 \leqslant (r/a)_{crit} \leqslant 1.12$ was found with the highest value of 1.12 being obtained with the smallest and biggest indentors, of $R = 3$ and 10 mm, respectively. The average was $(r/a)_{crit} = 1.10$. For the subsequent calculations, the value 1.10 ± 0.03 was therefore used, regardless of R.

5. Discussion

The present results on Hertzian ring crack formation in ThO_2 can be used to deduce values of fracture surface energy, γ, and of fracture toughness, K_{IC}. Applying Equation 3 and taking the values of $k/(1-\nu^2)$ and of the crack extension function $(a/c'')[\phi'']^{-2}$ from Figs. 3 and 4, a value for γ is obtained:

$$\gamma = (2.5 \pm 0.2)\,\mathrm{J\,m^{-2}}.$$

The relation [5]

$$2\gamma = \frac{(1-\nu^2)}{E} K_{IC}^2 \qquad (4)$$

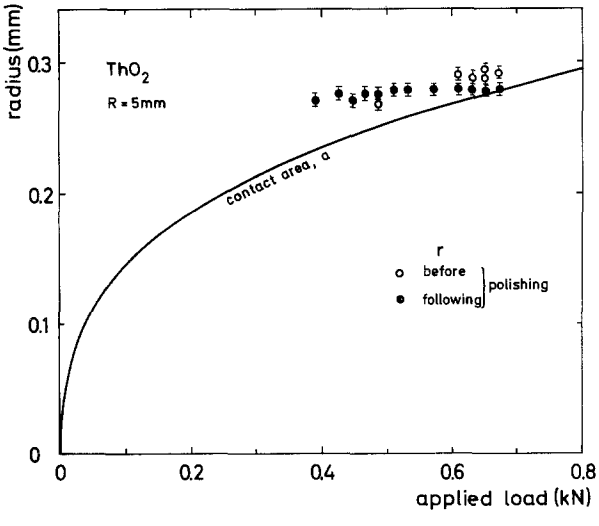

Figure 12 Measured crack radii, r, compared to the calculated contact area, a, for cracking at increasing load with $R = 5$ mm, before and following polishing the surface with 1 μm diamond paste.

allows calculations of the fracture toughness. The value for K_{IC} is 1.07 MN m$^{-3/2}$.

No published value of the fracture surface energy of ThO_2 could be found to make comparisons with the present results. Calculated values [24] of the surface energy of equilibrium {1 1 1} faces at 0 K of 0.81 or 1.15 J m^{-2} are very sensitive to polarizabilities, ionic radii, Pauling factors, and compressibilities used. A 10% variation of the compressibility, for instance, causes a change in calculated surface energy of 0.3 J m^{-2}. The same calculation led also to a very low value of 0.15 J m^{-2} for UO_2.

Comparison with the high temperature data for UO_2 obtained predominantly by wetting and multi-phase equilibration techniques (e.g. [1–3, 25]) and yielding values between about 0.2 and 1.0 J m^{-2} depending on O/U ratio and temperature, seems premature. Firstly, the high temperature surfaces are both relaxed and often polarized [26] whereas the present results represent the surface before relaxation and polarization. The high temperature equilibrium data are expected to be lower [26] and cannot *a priori* be compared with the present results. Secondly, there is still a dispute on the effect of deviations from stoichiometry and the truely representative value for stoichiometric UO_2 (e.g. [3, 27]). More work is needed to solve these open questions.

Furthermore, values of the fracture surface energy obtained by Hertzian indentation may be high. In addition to the uncertainty introduced by the approximate nature of the fracture analysis two other possible explanations exist to explain high values of γ.

(i) A first possibility is that the indentation value is high due to deviation from purely elastic behaviour. Plastic deformation of the sample beneath the indentor prior to cracking would lead to a higher cracking load and consequently to an overestimation of γ. Such deformation would yield permanent indentation. Alternatively, the actual crack formation may involve some localized short-range yielding. Such plasticity would be an intrinsic and valid part of the fracture surface energy, and it would not lead to significant deviation from Hertzian elastic indentation.

In the present study, however, no sign of plastic deformation could be observed for indentors with $R \geqslant 2.5$ mm. Smaller indentors ($R = 0.5$ or 1 mm) did yield plastic indentations (see Fig. 5). This is consistent with the observations of Evans and Wilshaw [28] that there is a transition from plastic to elastic indentation behaviour as R is increased.

(ii) A second possibility is that the indentation crack deviates locally from a perfect circle (cone), e.g. by seeking out suitably located pores or by branching, and the effective surface area is thereby increased. A large true surface area was suggested to partly explain the high effective surface energy of fracture initiation, γ_i, measured by Evans and Davidge for UO_2 [29].

However, measurements by Warren on carbides indicated that in seeking out pores the ring crack gains about as much as it loses [5] and in fact he suggested that in order to obtain γ for the pore-free material the experimental value of γ should simply be corrected upwards by a factor of $1/(1-P)$, where P is the volume fraction porosity. Such a correction may be an unnecessary over-refinement in view of other possible complications introduced by porosity. For instance, gas pressure remaining in the pores and causing stresses might compensate this correction, or crack extension further than to the (calculated) depth because of the tendency of cracks to reach closed pores might increase the total surface area.

6. Conclusions

The technique of Hertzian indentation was shown to yield a consistent value of fracture surface energy, γ, of 2.5 ± 0.2 J m^{-2} for sintered ThO_2 at room temperature for a wide range of indentor radii (3 to 10 mm). No indication of permanent plastic deformation was observed. The technique to observe ring cracks was refined by slight mechanical polishing of the samples before observation in the optical microscope, and by applying acoustic emission. It could be shown that the cone cracks form on loading and when the critical load is reached, even if overloads are applied for a longer time. The fracture toughness, $K_{IC} = 1.07$ MN m$^{-3/2}$ of sintered ThO_2 at room temperature could also be deduced from the present data.

Acknowledgements

The author would like to thank Dr R. Warren (Chalmers Technical University, Göteborg, Sweden) for many discussions and for making his results available before publication. He is also grateful to Miss W. Millington (University of Surrey, UK), T. Inoue (CRIEPI, Tokio) and V. Meyritz for experimental help.

References

1. E. N. HODKIN and M. G. NICHOLAS, *J. Nucl. Mater.* **67** (1977) 171.
2. P. NIKOLOPOULOS, S. NAZARÉ and F. THÜMMLER, *ibid.* **71** (1977) 89.
3. E. N. HODKIN and M. G. NICHOLAS, *ibid.* **74** (1978) 178.
4. H. HERTZ, in "Hertz's Miscellaneous Papers" (MacMillan, London, 1896) Ch. 5, 6.
5. R. WARREN, *Acta Met.* **26** (1978) 1759.
6. Hj. MATZKE and R. WARREN, *J. Nucl. Mater.*, submitted.
7. Hj. MATZKE and C. POLITIS, *Phys. Stat. Sol.*, submitted.
8. F. AUERBACH, *Ann. Phys. Chem.* **43** (1891) 61.
9. A. A. GRIFFITH, *Phil. Trans. Roy. Soc. London A* **221** (1920) 163.
10. F. C. ROESLER, *Proc. Phys. Soc. (London)* **B69** (1956) 55.
11. B. R. LAWN and R. WILSHAW, *J. Mat. Sci.* **10** (1975) 1049.
12. I. FINNIE and S. VAIDYANATHAN, in "Fracture Mechanisms of Ceramics", Vol. 3, edited by R. C. Bradt, D. P. H. Hasselman and F. F. Lange (Plenum Publishing Corporation, New York, 1978) p. 205.
13. B. D. POWELL and D. TABOR, *J. Phys. D: Appl. Phys.* **3** (1970) 783.
14. F. B. LANGITAN and B. R. LAWN, *J. Appl. Phys.* **40** (1969) 4009.
15. S. SPINNER, F. P. KNUDSEN and L. STONE, *J. Res. Nat. Bur. Stand. C. Eng. Instrum.* **67C** (1963) 39.
16. P. M. MACEDO, W. CAPPS and J. B. WACHTMAN Jr, *J. Amer. Ceram. Soc.* **57** (1964) 651.
17. J. B. WACHTMAN Jr, W. E. TEFFT, D. G. LAM and C. S. APSTEIN, *Phys. Rev.* **122** (1961) 1754.
18. S. M. LANG and F. P. KNUDSEN, *J. Amer. Ceram. Soc.* **39** (1956) 415.
19. D. R. OLANDER, Fundamental Aspects of Nuclear Reactor Fuels, US ERDA-Report TID-26711-P1 (1977).
20. M. O. MARLOWE and A. I. KAZNOFF, "Proceedings of the International Symposium on Ceramic Nuclear Fuels" (Amer. Ceram. Soc., Washington, 1969).
21. M. O. MARLOWE, *J. Nucl. Mater.* **33** (1969) 242.
22. A. PADEL and CH. DE NOVION, *ibid.* **33** (1969) 40.
23. C. POLITIS, KfK Karlsruhe, personal communication (1978).
24. G. C. BENSON, P. I. FREEMAN and E. DEMPSEY, *J. Amer. Ceram. Soc.* **46** (1963) 43.
25. P. NIKOLOPOULOS, German Report KfK-2038 (1974).
26. G. C. BENSON, P. BALK and P. WHITE, *J. Phys. Chem.* **31** (1959) 109.
27. P. NIKOLOPOULOS, S. NAZARÉ and F. THÜMMLER, *J. Nucl. Mater.* **78** (1978) 213.
28. A. G. EVANS and T. R. WILSHAW, *Acta Met.* **24** (1976) 939.
29. A. G. EVANS and R. W. DAVIDGE, *J. Nucl. Mater.* **33** (1969) 249.

Received 10 July and accepted 26 July 1979.